Supramolecular polymers with tunable topologies via hierarchical coordination-driven self-assembly and hydrogen bonding interfaces

A Submission to the Proceedings of the National Academy of Science USA

PHYSICAL SCIENCES: Chemistry

Xuzhou Yan,[a,b] Shijun Li,[b,c] J. Bryant Pollock,[b] Timothy R. Cook,[b] Jianzhuang Chen,[a] Yanyan Zhang,[d] Xiaofan Ji,[a] Yihua Yu,[d] Feihe Huang,[a,1] and Peter, J. Stang[b,1]

[a]MOE Key Laboratory of Macromolecular Synthesis and Functionalization, Department of Chemistry, Zhejiang University, Hangzhou 310027, P. R. China
[b]Department of Chemistry, University of Utah, 315 South 1400 East, Room 2020, Salt Lake City, Utah 84112, United States
[c]College of Material, Chemistry and Chemical Engineering, Hangzhou Normal University, Hangzhou 310036, P. R. China
[d]Shanghai Key Laboratory of Magnetic Resonance, Department of Physics, East China Normal University, Shanghai 200062, P. R. China
[1]To whom correspondence should be addressed. Email address: stang@chem.utah.edu; fhuang@zju.edu.cn

Table of Contents (25 Pages)

Section A. Materials/General Methods/Instrumentation

All reagents were commercially available and used as supplied without further purification. Deuterated solvents

were purchased from Cambridge Isotope Laboratory (Andover, MA). Compounds **5** (S1), **6** (S2), **7**,[S2] **8**,[S3] **14**[S4], and parent rhomboid **15**[S8] were prepared according to the published procedures. NMR spectra were recorded on a Varian Unity 300 MHz spectrometer. ^{1}H and ^{13}C NMR chemical shifts are reported relative to residual solvent signals, and ^{31}P{^{1}H} NMR chemical shifts are referenced to an external unlocked sample of 85% H_3PO_4 (δ 0.0). The two-dimensional diffusion-ordered (2D DOSY) NMR spectra were recorded on a Bruker DRX500 spectrometer. Dynamic light scattering (DLS) was carried out on a Malvern Nanosizer S instrument at room temperature. FT-IR spectra were recorded on a NEXUS 47 FT-IR spectrometer. SEM investigations were carried out on a JEOL 6390LV instrument. TEM images were obtained using a Philips TECNAI-12 instrument with an accelerating voltage of 120 kV. Mass spectra were recorded on a Micromass Quattro II triple-quadrupole mass spectrometer using electrospray ionization with a MassLynx operating system. The melting points were collected on a SHPSIC WRS-2 automatic melting point apparatus.

Section B. Synthetic Protocols

*1. Synthesis of 120° UPy-functionalized ligand **4***

*1.1. Synthesis of compound **9***

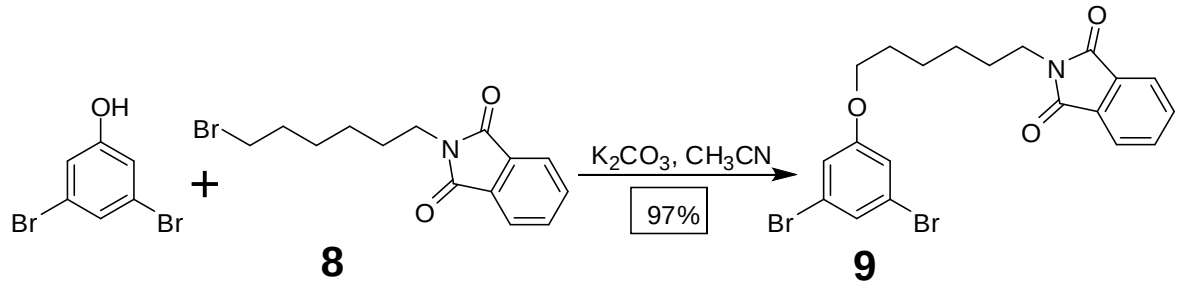

Into a 200 mL round-bottomed flask were added 3,5-dibromophenol (1.26 g, 5.00 mmol), **8** (2.02 g, 6.50 mmol), and K_2CO_3 (1.38 g, 10.0 mmol) in 100 mL of CH_3CN. After heating at reflux under N_2 for 12 h, the solvent was removed and CH_2Cl_2 was added. The mixture was washed with water and brine, and then purified by flash column chromatography (ethyl acetate/hexane, 1:5 *v*/*v*) to afford **9** as a white solid (2.33 g, 97%). Mp 126.7–128.3 °C. The ^{1}H NMR spectrum of **9** is shown in Figure S1. ^{1}H NMR ($CDCl_3$, room temperature, 300 MHz) δ (ppm): 7.82–7.85 (m, 2H), 7.69–7.72 (m, 2H), 7.21 (t, J = 1.6 Hz, 1H), 6.95 (d, J = 1.5 Hz, 2H), 3.89 (t, J = 6.5 Hz, 2H), 3.69 (t, J = 7.1 Hz, 2H), 1.64–1.81 (m, 4H), 1.33–1.53 (m, 4H). The ^{13}C NMR spectrum of **9** is shown in Figure S2. ^{13}C NMR ($CDCl_3$, room temperature, 75 MHz) δ (ppm): 25.26, 26.71, 28.69, 29.03, 38.06, 68.59, 117.11, 123.26, 123.41, 126.38, 132.33, 134.13, 160.47, and 168.69. LRESIMS is shown in Figure S3: *m*/*z* 503.7 $[M + Na]^+$. HRESIMS: *m*/*z* calcd for $[M + Na]^+$ $C_{20}H_{19}Br_2NNaO_3$, 503.9609; found 503.9611, error 0.30 ppm.

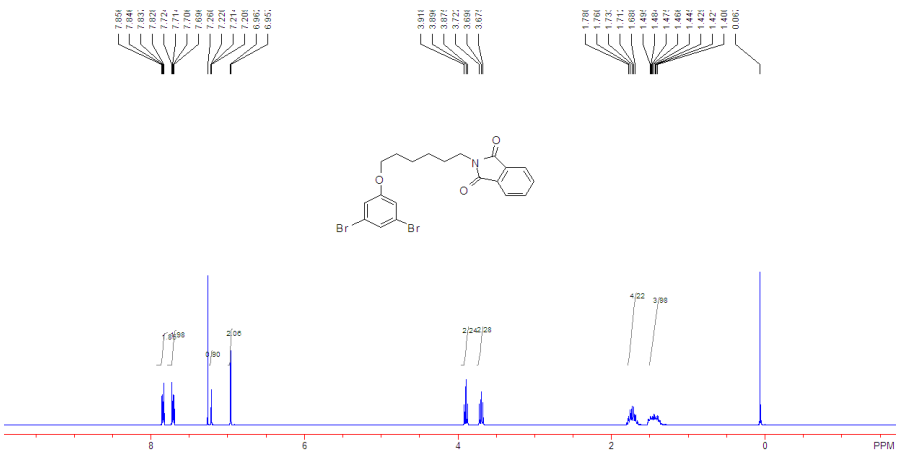

Figure S1. ^{1}H NMR spectrum ($CDCl_3$, room temperature, 300 MHz) of **9**.

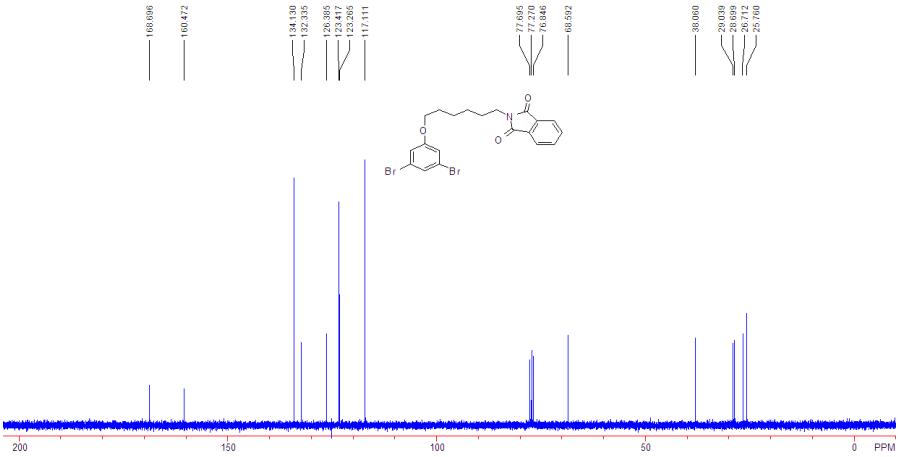

Figure S2. ^{13}C NMR spectrum ($CDCl_3$, room temperature, 75 MHz) of **9**.

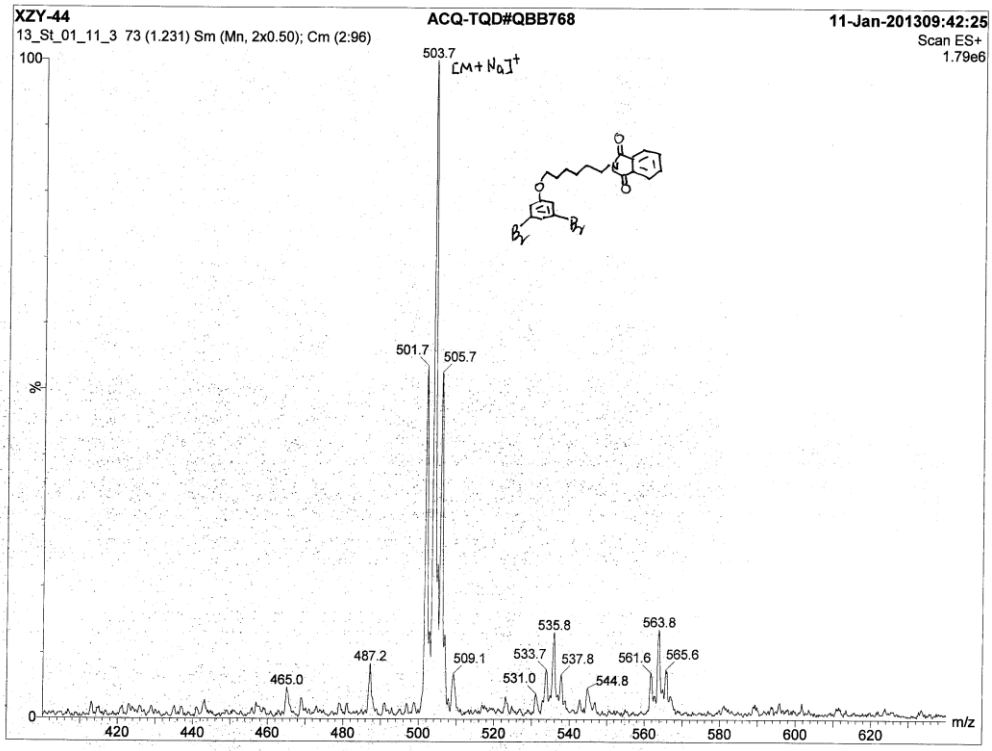

Figure S3. Electrospray ionization mass spectrum of **9**.

*1.2. Synthesis of compound **10***

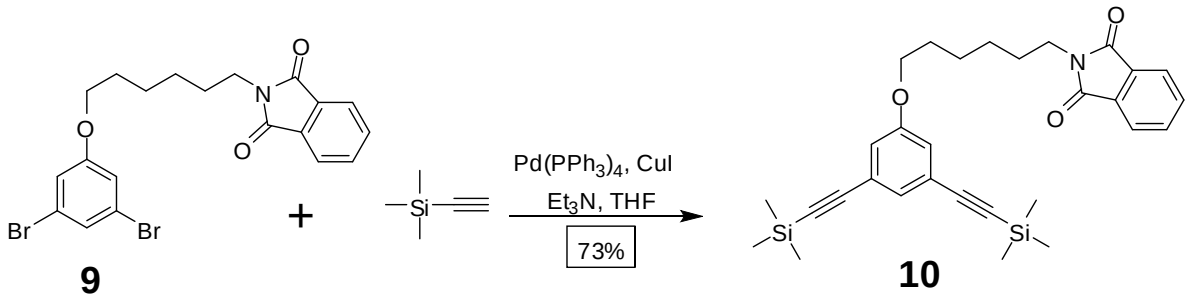

In a 100 mL round-bottom Schlenk flask, compound **9** (1.04 g, 2.16 mmol) and (trimethylsily)acetylene (1.27 g, 13.0 mmol) were dissolved in 60 mL of freshly distilled THF and 3.62 mL of dry triethylamine. Then, a mixture of tetrakis(triphenylphosphine)palladium (127 mg, 0.110 mmol) and cuprous iodide (17.0 mg, 0.0900 mmol) was added under a stream of N_2, and the suspension was stirred at 60 ºC for 24 h in the absence of light. After removal of the solvent, the residue was suspended in ethyl acetate and washed twice with water, and then purified by flash column chromatography (ethyl acetate/hexane, 1:50 *v*/*v*) to afford **10** as a pale yellow oil (0.780 g, 73%). The ^{1}H NMR spectrum of **10** is shown in Figure S4. ^{1}H NMR ($CDCl_3$, room temperature, 300 MHz) δ (ppm): 7.81–7.86 (m, 2H), 7.68–7.72 (m, 2H), 7.15 (t, J = 1.4 Hz, 1H), 6.90 (d, J = 1.5 Hz, 2H), 3.89 (t, J = 6.5 Hz, 2H), 3.69 (t, J = 7.2 Hz, 2H), 1.63–1.80 (m, 4H), 1.34–1.54 (m, 4H), 0.22 (s, 18H). The ^{13}C NMR spectrum of **10** is shown in Figure S5. ^{13}C NMR ($CDCl_3$, room temperature, 75 MHz) δ (ppm): 0.12, 25.82, 26.76, 28.73, 29.18, 38.10, 68.16, 94.72, 104.32, 118.45, 123.41, 124.35, 128.22, 132.34, 134.10, 158.69, and 168.69. LRESIMS is shown in Figure S6: *m*/*z* 516.0 $[M + H]^+$, 538.0 $[M + Na]^+$. HRESIMS: *m*/*z* calcd for $[M + Na]^+$ $C_{30}H_{37}NNaO_3Si_2$, 538.2210; found 538.2217, error 1.3 ppm.

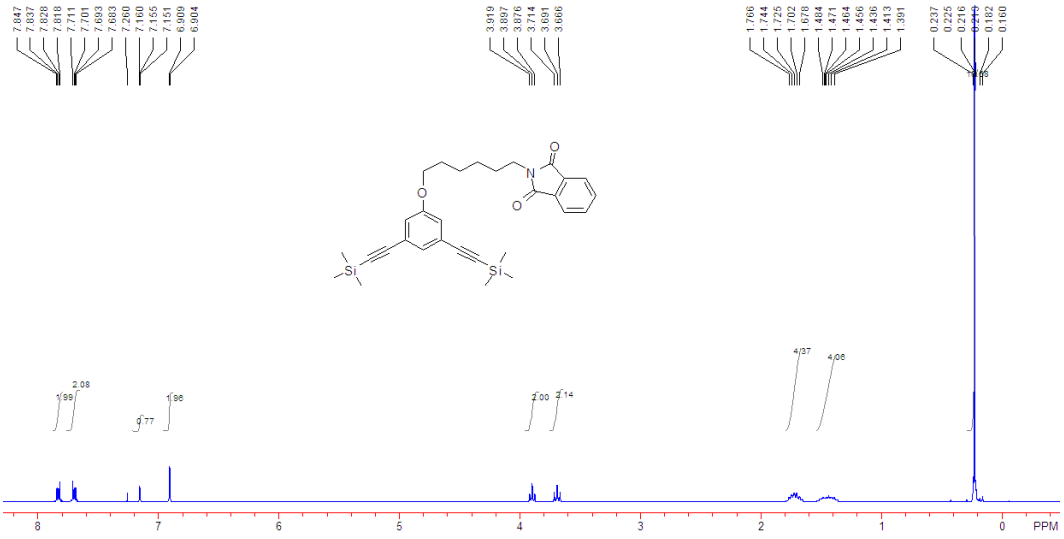

Figure S4. ^{1}H NMR spectrum ($CDCl_3$, room temperature, 300 MHz) of **10**.

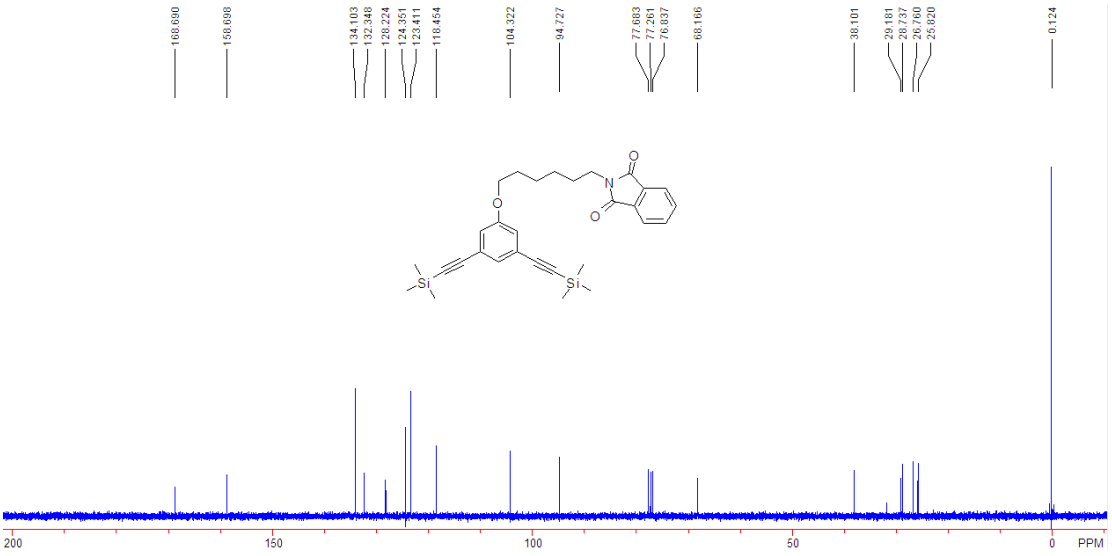

Figure S5. ^{13}C NMR spectrum ($CDCl_3$, room temperature, 75 MHz) of **10**.

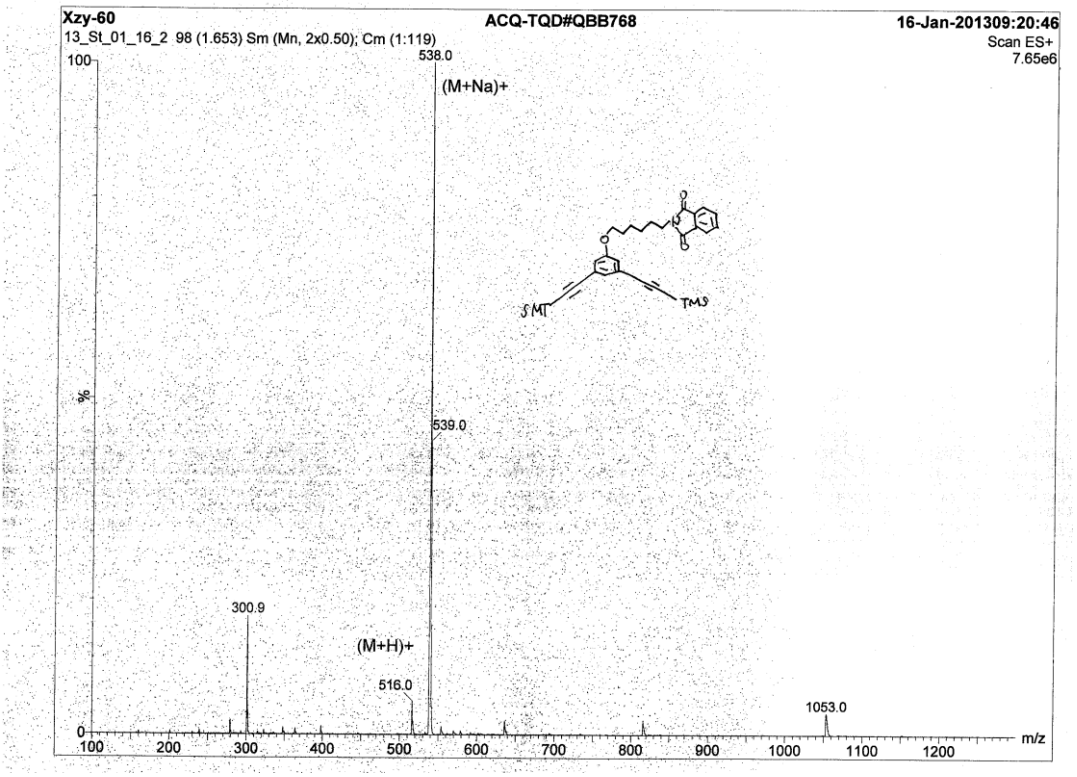

Figure S6. Electrospray ionization mass spectrum of **10**.

*1.3. Synthesis of compound **11***

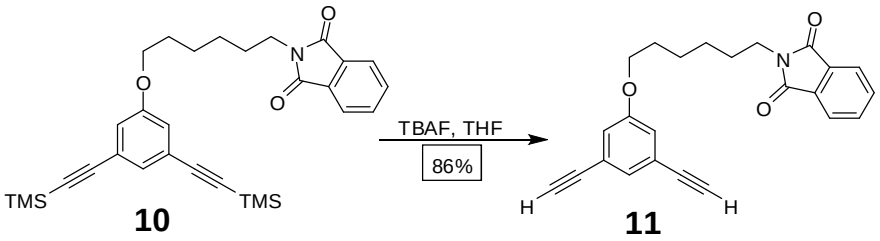

A solution of compound **10** (0.780 g, 1.51 mmol) in THF (20 mL) was treated with TBAF (1.0 M solution in THF, 3.03 mL, 3.03 mmol). The mixture was stirred at room temperature for 1 h and the solvent was removed under reduced pressure. Further purification by flash column chromatography (ethyl acetate/hexane, 1:20 *v*/*v*) afforded **11** as a white solid (0.620 g, 86%). Mp 102.8–103.5 °C. The ^{1}H NMR spectrum of **11** is shown in Figure S7. ^{1}H NMR ($CDCl_3$, room temperature, 300 MHz) δ (ppm): 7.78–7.85 (m, 2H), 7.65–7.72 (m, 2H), 7.16 (s, 1H), 6.95 s, 2H), 3.89 (t, J = 6.5 Hz, 2H), 3.68 (t, J = 7.2 Hz, 2H), 3.05 (s, 2H), 1.60–1.82 (m, 4H), 1.31–1.55 (m, 4H). The ^{13}C NMR spectrum of **11** is shown in Figure S8. ^{13}C NMR ($CDCl_3$, room temperature, 75 MHz) δ (ppm): 25.80, 26.76, 28.72, 29.14, 38.08, 68.24, 77.86, 82.84, 119.00, 123.39, 123.49, 128.25, 132.33, 134.10, 158.79, and 168.67. LRESIMS is shown in Figure S9: *m*/*z* 394.0 $[M + Na]^+$, 765.1 $[2M + Na]^+$. HRESIMS: *m*/*z* calcd for $[M + H]^+$ $C_{24}H_{22}NO_3$, 372.1600; found 372.1599, error –0.30 ppm.

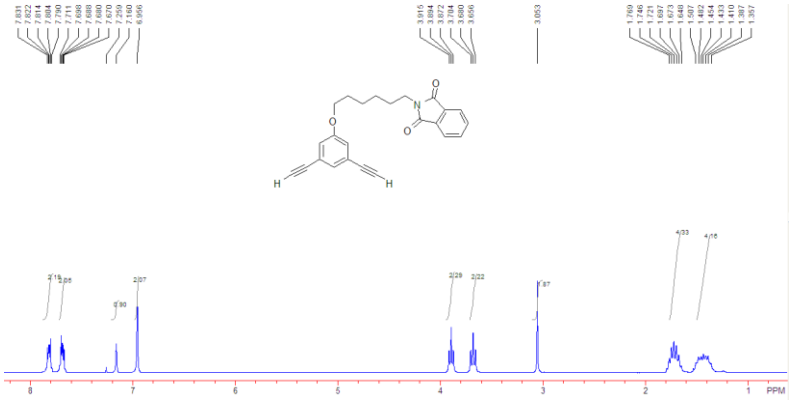

Figure S7. ^{1}H NMR spectrum ($CDCl_3$, room temperature, 300 MHz) of **11**.

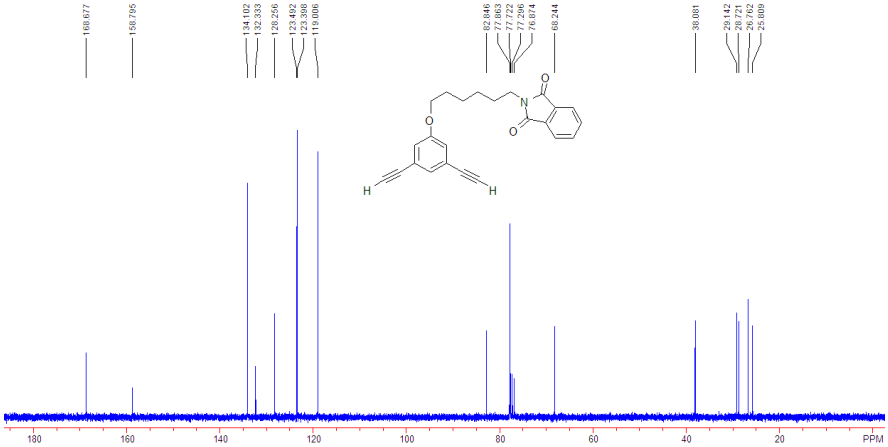

Figure S8. ^{13}C NMR spectrum ($CDCl_3$, room temperature, 75 MHz) of **11**.

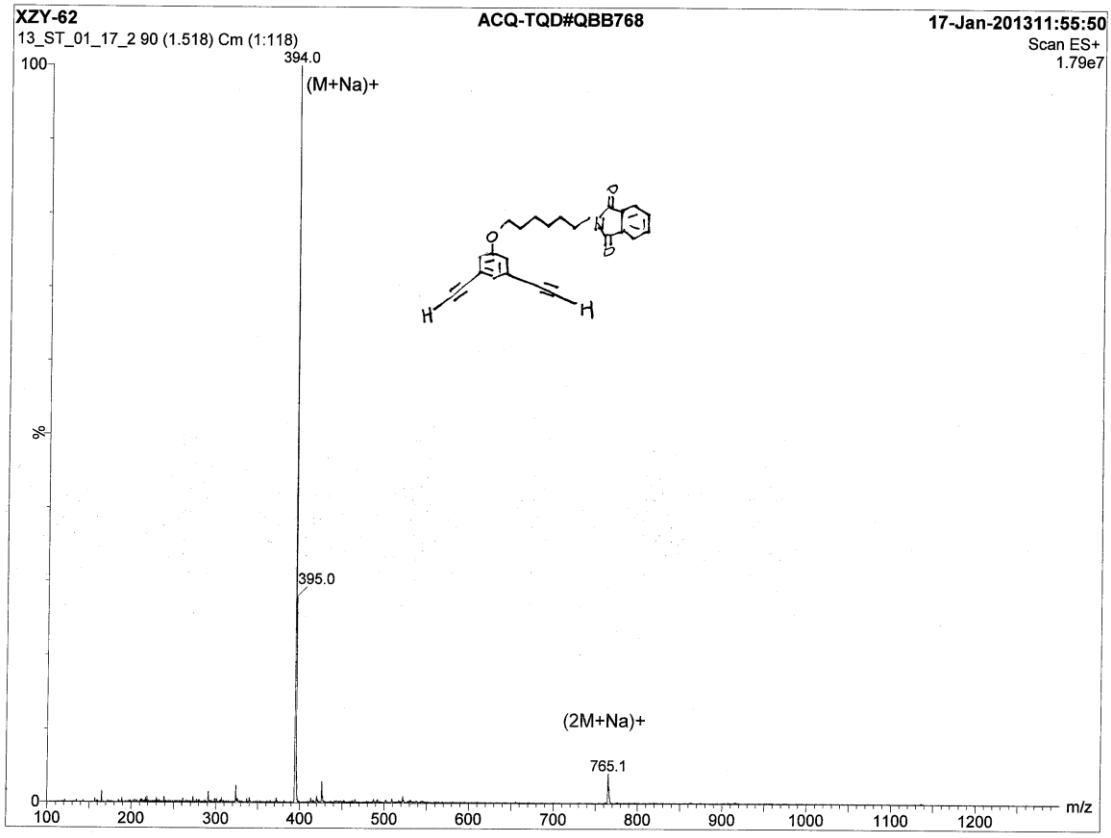

Figure S9. Electrospray ionization mass spectrum of **11**.

*1.4. Synthesis of compound **12***

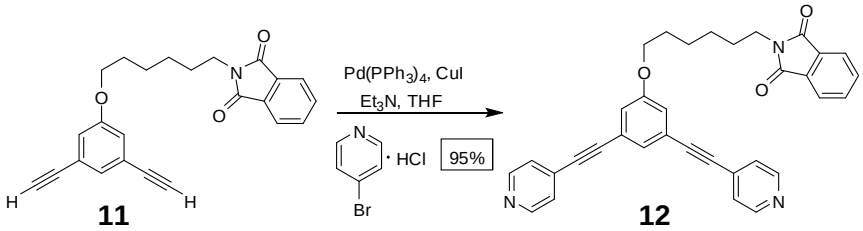

Into a 100 mL round-bottom Schlenk flask, compound **11** (0.742 g, 2.00 mmol), 4-bromopyridine hydrochloride (1.56 g, 8.00 mmol), tetrakis(triphenylphosphine)palladium (116 mg, 0.100 mmol), and cuprous iodide (16.0 mg, 0.080 mmol) were added. Freshly distilled THF (40 mL) and dry triethylamine (4 mL) were added to the flask *via* a syringe under N_2. The mixture was stirred at 60 °C for 24h. After removal of the solvent, the residue was suspended in ethyl acetate and washed twice with water, and then purified by flash column chromatography (CH_2Cl_2/MeOH, 100:1 *v*/*v*) to afford **12** as a brown solid (0.997 g, 95%). Mp 129.8–131.2 °C. The ^{1}H NMR spectrum of **12** is shown in Figure S10. ^{1}H NMR ($CDCl_3$, room temperature, 300 MHz) δ (ppm): 8.60 (d, J = 6.0 Hz, 4H), 7.76–7.79 (m, 2H), 7.65–7.72 (m, 2H), 7.35–7.40 (m, 4H), 7.31 (s, 1H), 7.07 (d, J = 1.2 Hz, 2H), 3.97 (t, J = 6.3 Hz, 2H), 3.69 (t, J = 7.2 Hz, 2H), 1.64–1.84 (m, 4H), 1.34–1.56 (m, 4H). The ^{13}C NMR spectrum of **12** is shown in Figure S11. ^{13}C NMR ($CDCl_3$, room temperature, 75 MHz) δ (ppm): 25.81, 26.75, 28.73, 29.14, 38.07, 68.40, 87.27, 93.04, 119.90, 123.41, 123.70, 125.80, 127.76, 128.64, 128.80, 131.31, 132.32, 134.13, 149.99,

159.08, and 168.70. LRESIMS is shown in Figure S12: *m/z* 263.6 $[M + 2H]^{2+}$, 526.0 $[M + H]^{+}$. HRESIMS: *m/z* calcd for $[M + H]^{+}$ $C_{34}H_{28}N_3O_3$, 526.2131; found 526.2144, error 2.4 ppm.

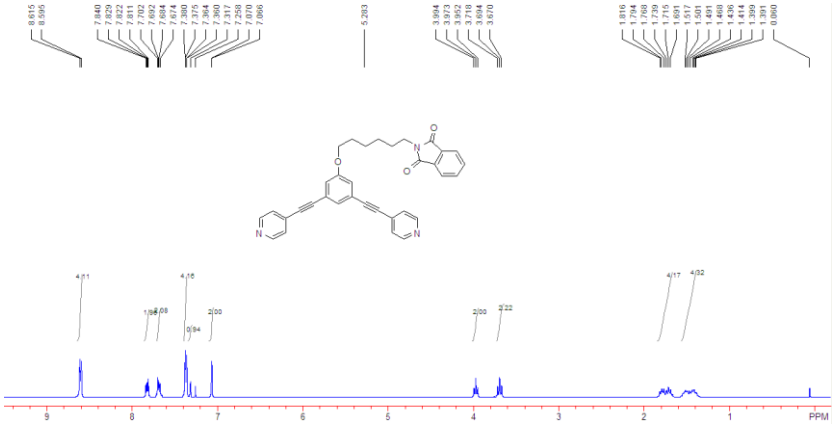

Figure S10. ^{1}H NMR spectrum ($CDCl_3$, room temperature, 300 MHz) of **12**.

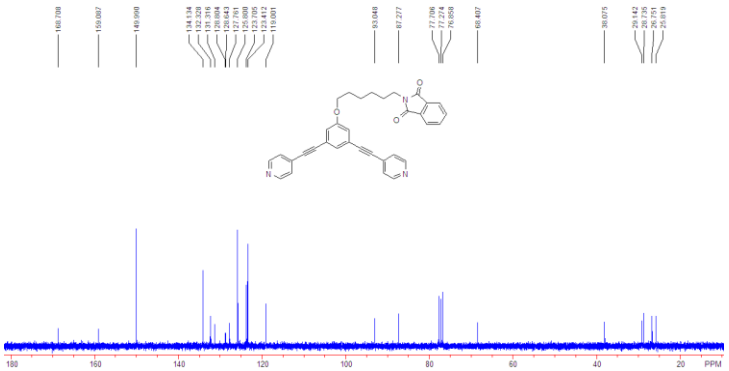

Figure S11. ^{13}C NMR spectrum ($CDCl_3$, room temperature, 75 MHz) of **12**.

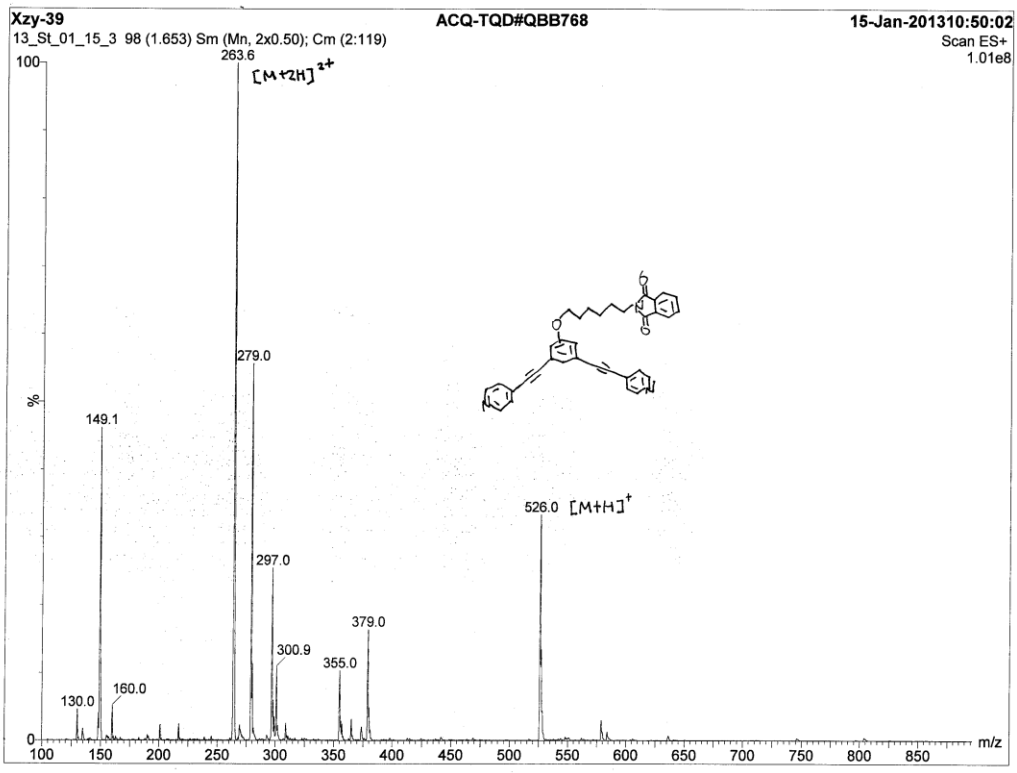

Figure S12. Electrospray ionization mass spectrum of **12**.

*1.5. Synthesis of compound **13***

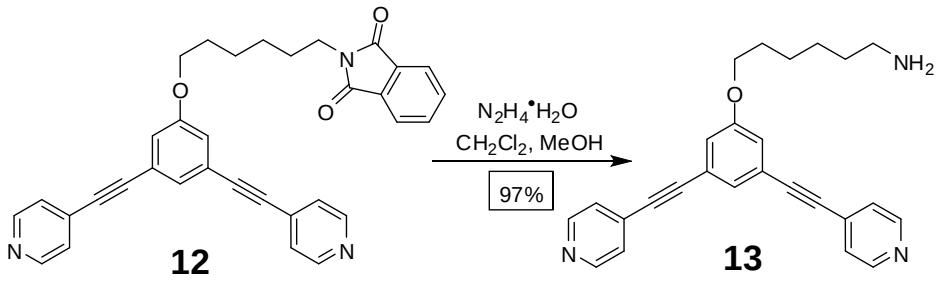

To a solution of compound **12** (1.50 g, 2.85 mmol) in CH_2Cl_2 (30 mL) and CH_3OH (50 mL) under N_2, hydrazine monohydrate was added and the mixture was stirred at 50 °C for 5h. After evaporation, the mixture was dissolved in chloroform and washed with 3M aqueous NaOH, water, brine and dried over anhydrous Na_2SO_4. After filtration, the solvent was removed under reduced pressure to afford **13** as pale yellow oil (1.10g, 97%). The ^{1}H NMR spectrum of **13** is shown in Figure S13. ^{1}H NMR ($CDCl_3$, room temperature, 300 MHz) δ (ppm): 8.57–8.62 (m, 4H), 7.33–7.38 (m, 4H), 7.65–7.72 (m, 2H), 7.32 (t, J = 1.4 Hz, 1H), 7.07 (d, J = 1.5 Hz, 2H), 3.98 (t, J = 6.5 Hz, 2H), 2.70 (t, J = 6.6 Hz, 2H), 1.75–1.86 (m, 2H), 1.35–1.51 (m, 6H). The ^{13}C NMR spectrum of **13** is shown in Figure S14. ^{13}C NMR ($CDCl_3$, room temperature, 75 MHz) δ (ppm): 26.10, 26.83, 29.29, 33.75, 42.30, 68.50, 87.29, 92.93, 118.96, 123.73, 125.76, 127.76, 131.21, 150.08, and 159.12. LRESIMS is shown in Figure S15: m/z 396.1 $[M + H]^+$, 791.2 $[2M + H]^+$. HRESIMS: m/z calcd for $[M + H]^+$ $C_{26}H_{26}N_3O$, 396.2076; found 396.2069, error –1.7 ppm.

Figure S13. ^{1}H NMR spectrum ($CDCl_3$, room temperature, 300 MHz) of **13**.

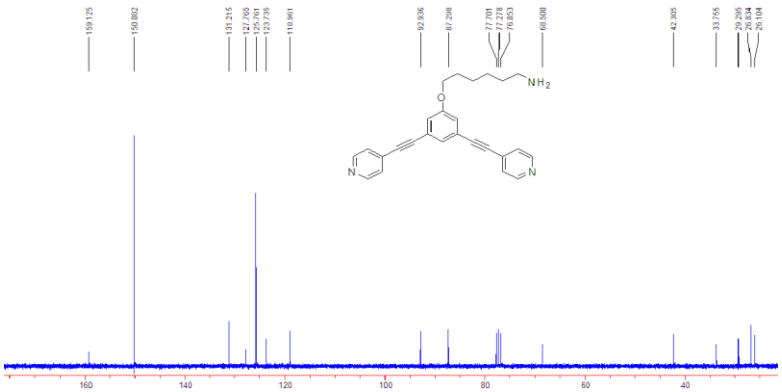

Figure S14. ^{13}C NMR spectrum ($CDCl_3$, room temperature, 75 MHz) of **13**.

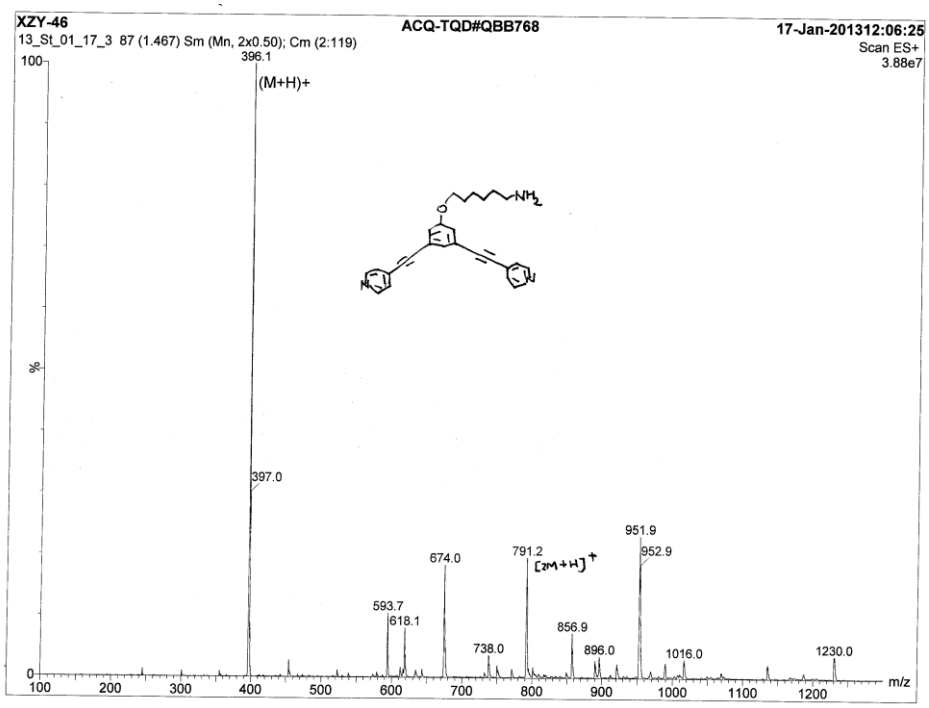

Figure S15. Electrospray ionization mass spectrum of **13**.

*1.6. Synthesis of compound **4***

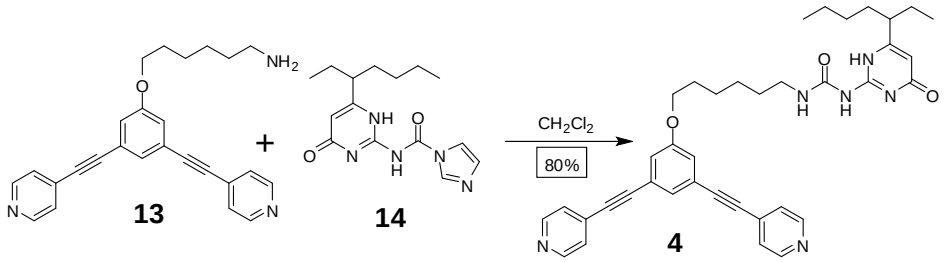

A solution of compound **13** (1.10 g, 2.78 mmol) and imidazolide **14** (1.69 g, 5.56 mmol) in dry CH_2Cl_2 (60 mL) was stirred for 3 h under N_2 at room temperature. To the reaction mixture, CH_2Cl_2 (40 mL) was added. The organic layer was washed with saturated $NaHCO_3$ and brine, and then dried over anhydrous Na_2SO_4. After removal of the solvent, the residue was purified by flash column chromatography (CH_2Cl_2/MeOH, 100:1 *v*/*v*) to afford **4** as a white solid (1.40 g, 80%). Mp 64.8–65.7 °C. The ^{1}H NMR spectrum of **4** is shown in Figure S16. ^{1}H NMR ($CDCl_3$, room temperature, 300 MHz) δ (ppm): 13.24 (s, 1H), 11.91 (s, 1H), 10.24 (s, 1H), 8.62 (s, 4H), 7.39 (t, J = 5.1 Hz, 4H), 7.32 (m, 1H), 7.07–7.09 (m, 2H), 5.80 (s, 1H), 3.98 (t, J = 6.3 Hz, 2H), 3.18–3.33 (m, 2H), 2.21–2.35 (m, 1H), 1.75–1.88 (m, 2H), 1.40–1.72 (m, 10H), 1.15–1.30 (m, 4H), 0.75–0.92 (m, 6H). The ^{13}C NMR spectrum of **4** is shown in Figure S17. ^{13}C NMR (DMSO-d_6, room temperature, 75 MHz) δ (ppm): 9.23, 12.48, 14.55, 22.87, 25.77, 26.68, 27.25, 29.07, 29.77, 33.72, 46.24, 68.71, 87.94, 92.88, 119.48, 123.71, 125.11, 126.09, 127.68, 130.46, 150.70, and 159.46. LRESIMS is shown in Figure S18: *m*/*z* 653.0 $[M + Na]^+$, 1283.2 $[2M + Na]^+$. HRESIMS: *m*/*z* calcd for $[M + Na]^+$ $C_{38}H_{42}N_6NaO_3$, 653.3216; found 653.3225, error 1.4 ppm.

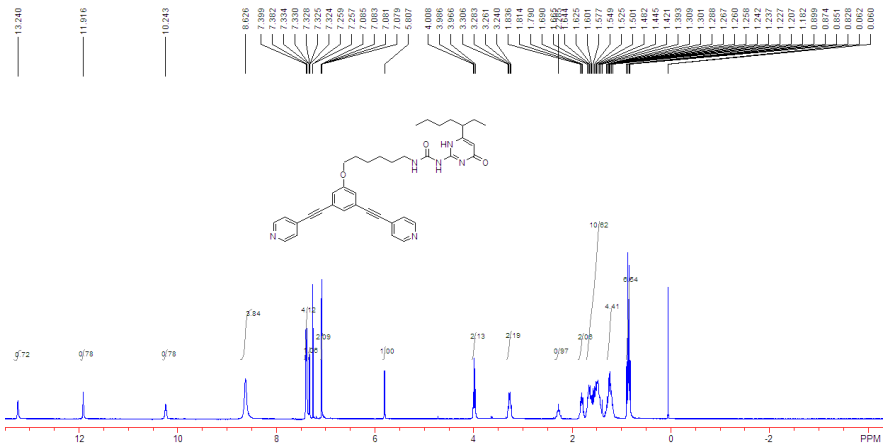

Figure S16. ^{1}H NMR spectrum ($CDCl_3$, room temperature, 300 MHz) of **4**.

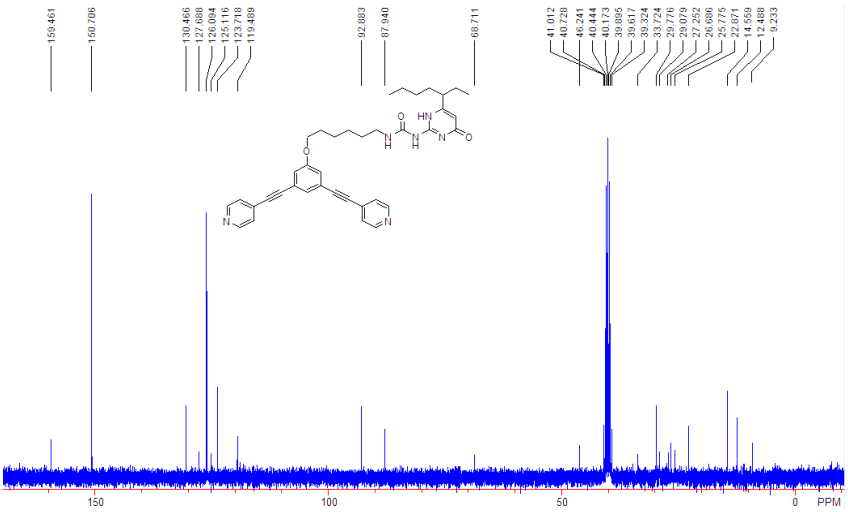

Figure S17. ^{13}C NMR spectrum (DMSO-d_6, room temperature, 75 MHz) of **4**.

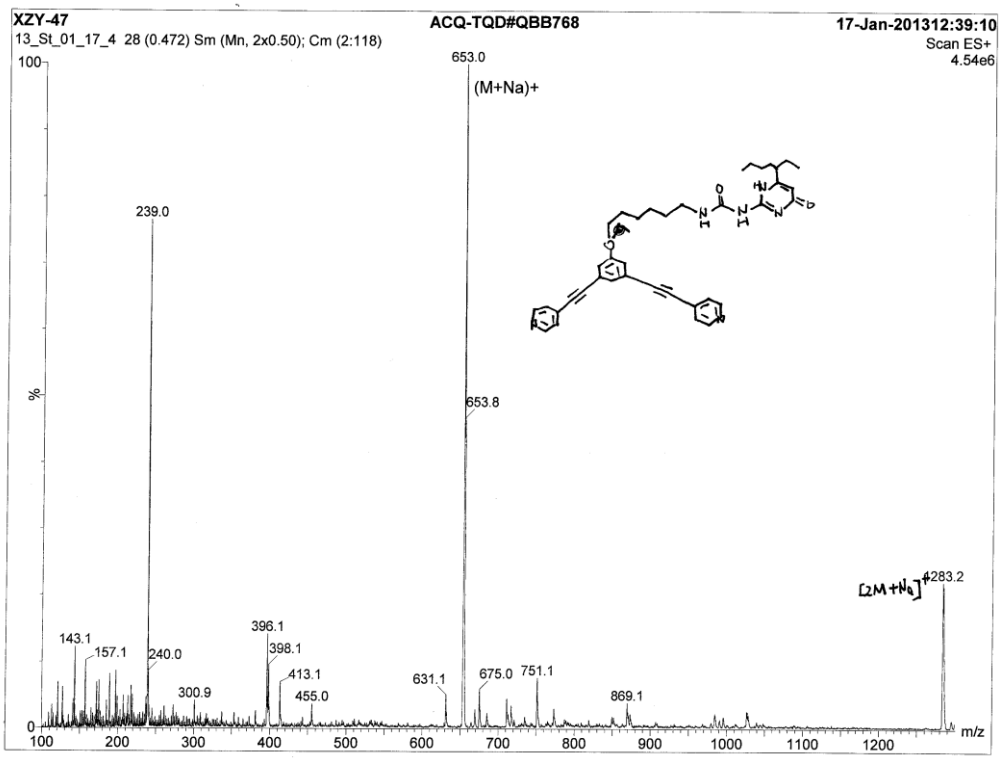

Figure S18. Electrospray ionization mass spectrum of **4**.

*2. Synthesis of UPy-functionalized rhomboid **1***

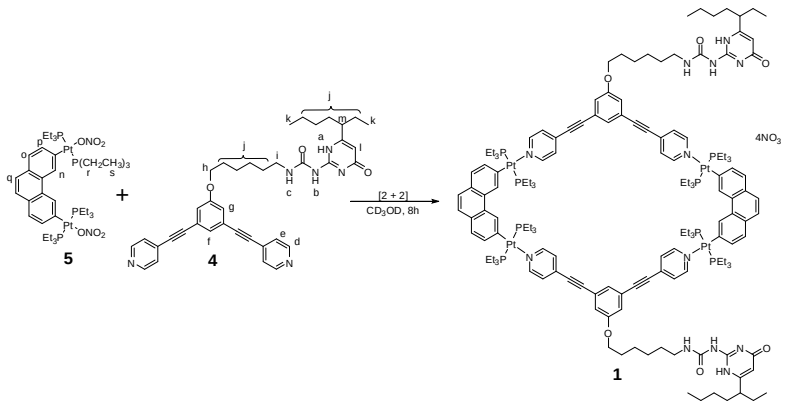

In a 1:1 molar ratio, 120° UPy-functionalized ligand **4** (1.89 mg, 0.003 mmol) and 60° 3,6-bis[*trans*-Pt(PEt_3)$_2$(NO_3)$_2$]phenanthrene **5** (3.49 mg, 0.003 mmol) were dissolved in 1.0 mL of CD_3OD in a 2 mL dram vial. The reaction mixture was allowed to stir for 8 h at 50 °C. To the resulting homogeneous solution, diethyl ether was added to precipitate the product, which was then isolated and dried under reduced pressure and re-dissolved in CD_3OD for characterization. The ^{1}H NMR spectrum of rhomboid **1** is shown in Figure S19. ^{1}H NMR (CD_3OD, room temperature, 300 MHz) δ (ppm): 9.02 (d, J = 5.7 Hz, 4H), 8.93 (d, J = 6.0 Hz, 4H), 8.67 (s, 4H), 7.94–8.00 (m, 4H), 7.84–9.00 (m, 4H), 7.70 (s, 4H), 7.65 (s, 2H), 7.62–7.64 (m, 4H), 7.58–7.61 (m, 4H), 7.35 (d, J = 1.2 Hz, 4H), 5.85 (s, 2H), 4.12 (t, J = 6.3 Hz, 4H), 2.26–2.42 (m, 2H), 1.80–1.96 (m, 4H), 1.53–1.73 (m, 32H), 1.35–1.52 (m, 48H), 1.10–1.30 (m, 72H), 0.76–0.93 (m, 12H). The ^{31}P {^{1}H} NMR spectrum of rhomboid **1** is shown in Figure S20. ^{31}P {^{1}H} NMR (CD_3OD, room temperature, 121.4 MHz) δ (ppm): 11.76 ppm (s, ^{195}Pt satellites, $^1J_{Pt-P}$ = 2676.4 Hz). ESI-MS is shown in Figure S21: m/z 834.85 $[M - 4NO_3]^{4+}$, 1112.81 $[M - HNO_3 - 3NO_3]^{3+}$, 1124.79 $[M - 2HNO_3 - 2NO_3 + K]^{3+}$, 1133.80 $[M - 3NO_3]^{3+}$, 1731.68 $[M - 2NO_3]^{2+}$.

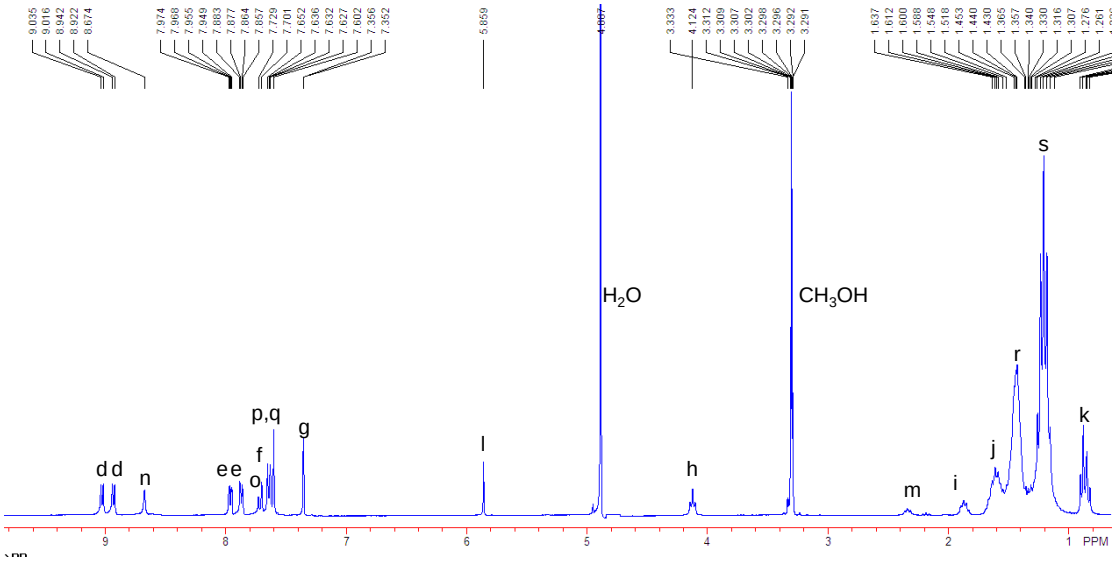

Figure S19. ^{1}H NMR spectrum (CD_3OD, room temperature, 300 MHz) of rhomboid **1**.

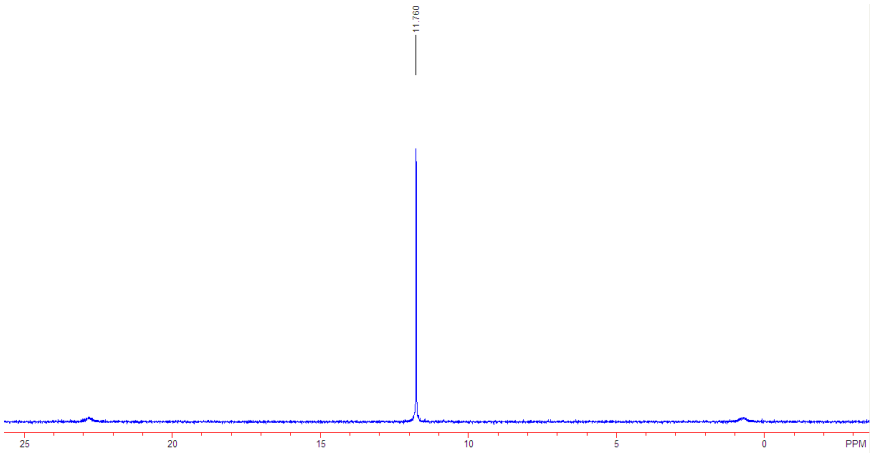

Figure S20. ^{31}P $\{^{1}H\}$ NMR spectrum (CD_3OD, room temperature, 121.4 MHz) of rhomboid **1**.

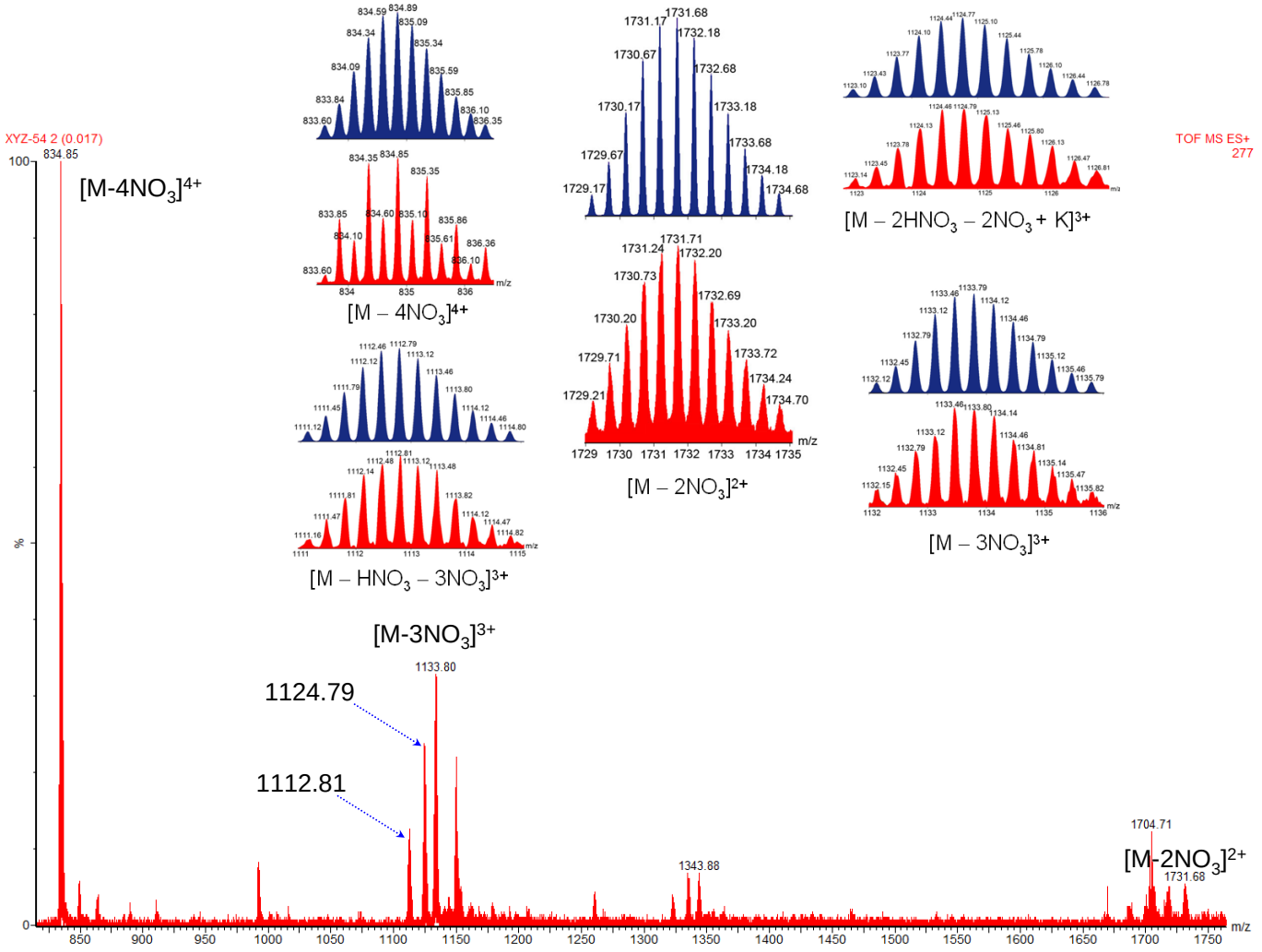

Figure S21. Experimental (red) and calculated (blue) electrospray ionization mass spectrum of rhomboid **1**.

*3. Synthesis of UPy-functionalized hexagon **2***

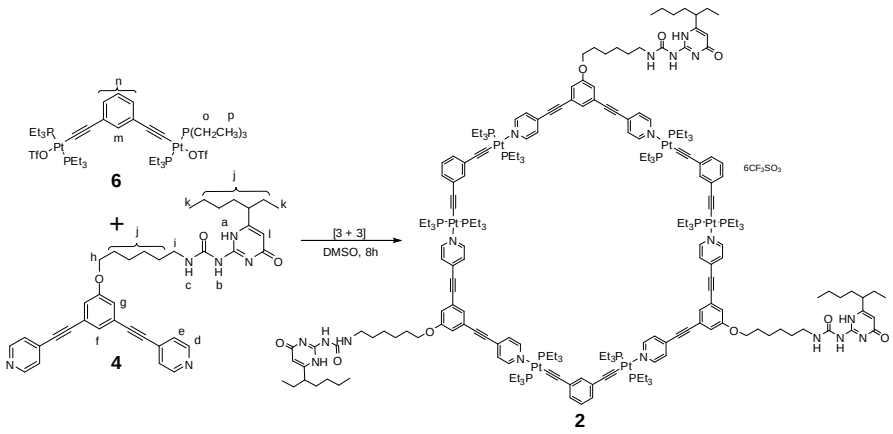

In a 1:1 molar ratio, 120° UPy-functionalized ligand **4** (1.89 mg, 0.003 mmol) and 120° 1,3-bis[*trans*-Pt(PEt$_3$)$_2$(OTf)$_2$ ethynyl]benzene **6** (3.86 mg, 0.003 mmol) were dissolved in 1.0 mL of DMSO-d_6 in a 2 mL dram vial. The reaction mixture was allowed to stir for 8 h at 50 °C. To the resulting homogeneous solution, diethyl ether was added to precipitate the product, which was then isolated and dried under reduced pressure and re-dissolved in DMSO-d_6 for characterization. The ^{1}H NMR spectrum of hexagon **2** is shown in Figure S22. ^{1}H NMR (DMSO-d_6, room temperature, 300 MHz) δ (ppm): 11.41 (s, 3H), 9.55 (s, 3H), 8.85 (d, J = 5.7 Hz, 12H), 7.81 (d, J = 5.4 Hz, 12H), 7.54 (s, 3H), 7.52 (s, 3H), 7.39 (d, J = 5.1 Hz, 6H), 6.97–7.12 (m, 12H), 5.71 (s, 3H), 3.97–4.14 (m, 6H), 3.09–3.19 (m, 6H), 1.65–1.90 (m, 72H), 1.29–1.56 (m, 51H), 0.95–1.18 (m, 108H), 0.67–0.85 (m, 18H). The ^{31}P {^{1}H} NMR spectrum of hexagon **2** is shown in Figure S23a. ^{31}P {^{1}H} NMR (DMSO-d_6, room temperature, 121.4 MHz) δ (ppm): 13.15 ppm (s, ^{195}Pt satellites, $^1J_{Pt–P}$ = 2309.5 Hz). ESI-MS is shown in Figure S24: *m*/*z* 808.84 [M – 6OTf]$^{6+}$, 818.34 [M – 2HOTf – 4OTf + Na + K]$^{6+}$, 970.41 [M – HOTf – 5OTf]$^{5+}$, 977.60 [M – 3HOTf – 3OTf + 2NH$_4$]$^{5+}$, 1000.40 [M – 5OTf]$^{5+}$, 1212.50 [M – 2HOTf – 4OTf]$^{4+}$, 1288.23 [M – 4OTf]$^{4+}$, 1628.65 [M – 4HOTf – 2OTf + K]$^{3+}$.

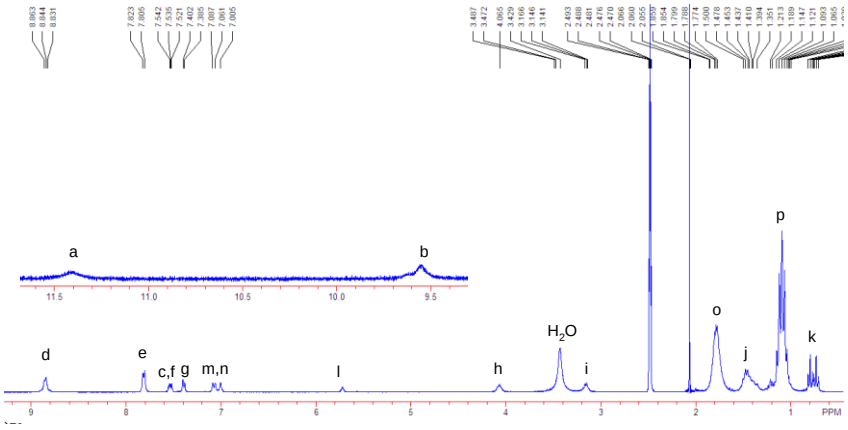

Figure S22. ^{1}H NMR spectrum (DMSO-d_6, room temperature, 300 MHz) of hexagon **2**.

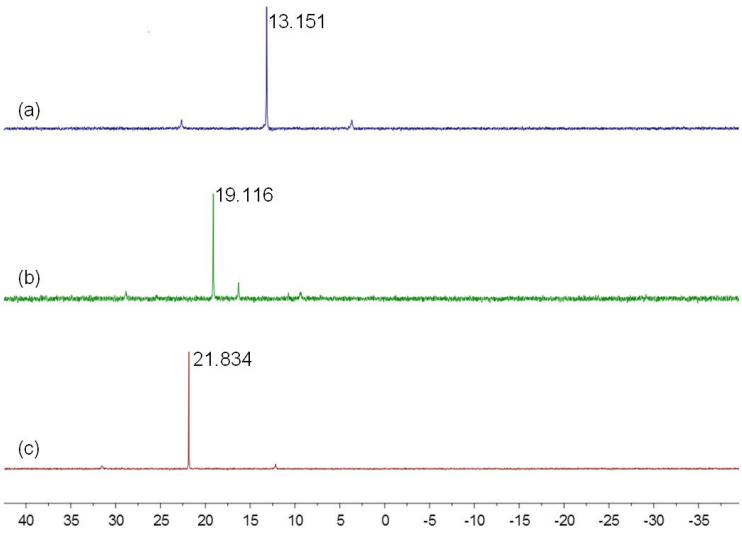

Figure S23. ^{31}P {^{1}H} NMR spectrum (room temperature, 121.4 MHz) of hexagon **2** in DMSO-d_6 (a), acceptor **6** in DMSO-d_6 (b), and acceptor **6** in CD_2Cl_2 (c). The impurity on spectrum b was caused by DMSO-d_6 because it can coordinate with acceptor **6**.

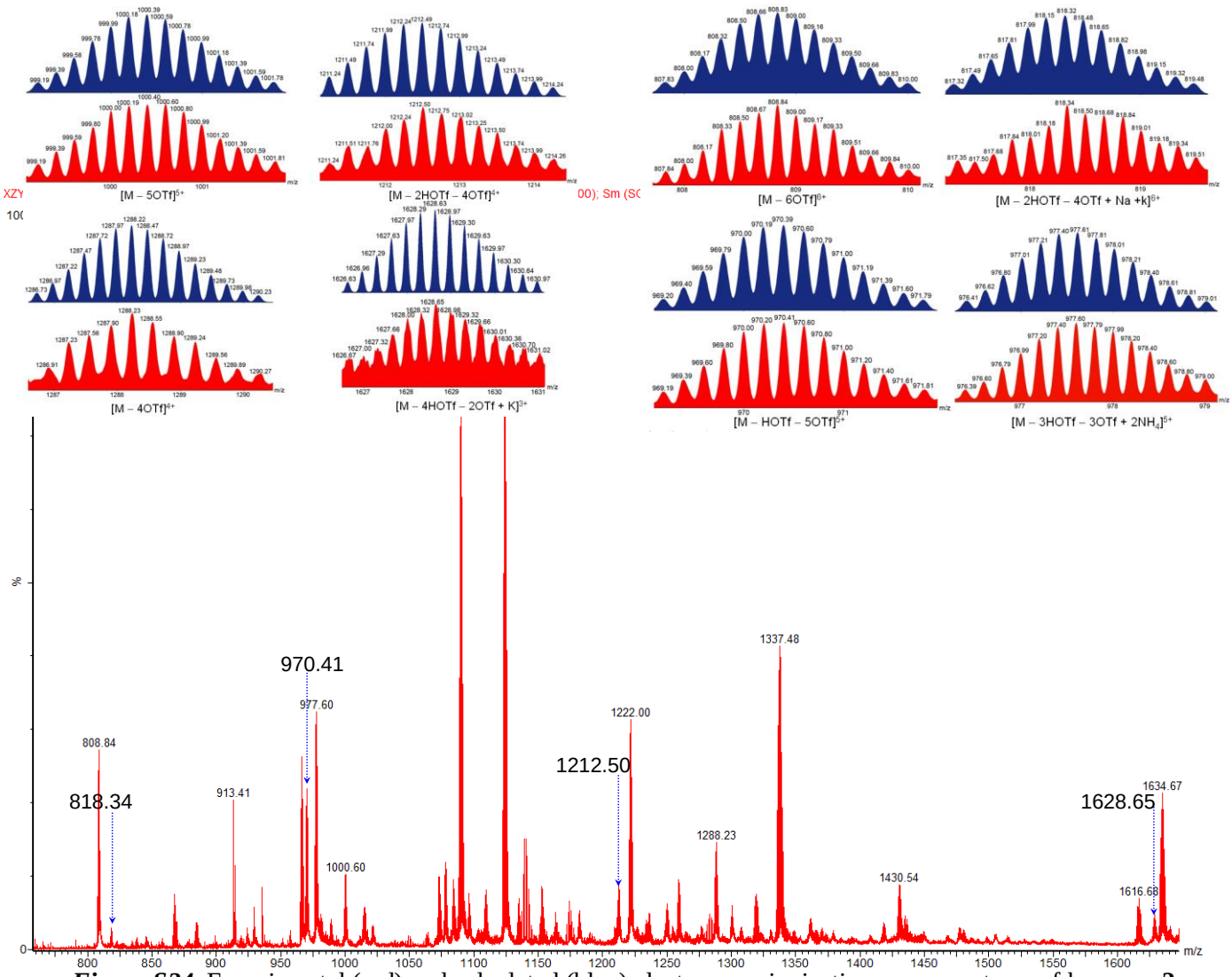

Figure S24. Experimental (red) and calculated (blue) electrospray ionization mass spectrum of hexagon **2**.

*4. Synthesis of UPy-functionalized hexagon **3***

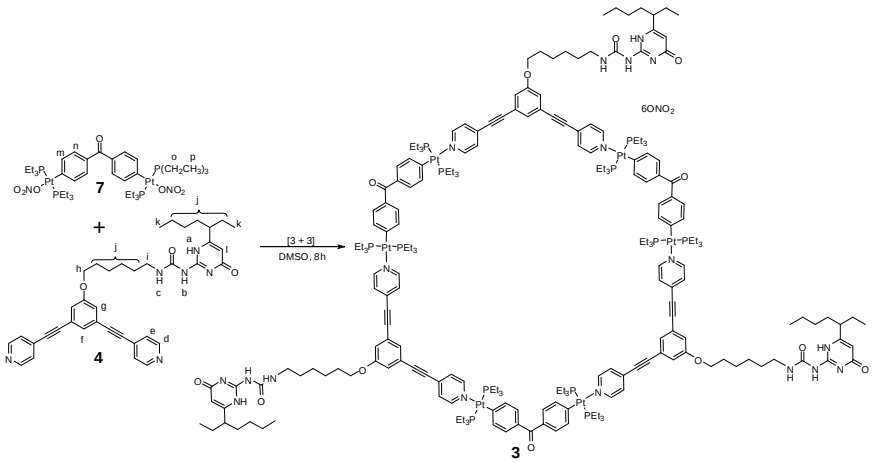

In a 1:1 molar ratio, 120° UPy-functionalized ligand **4** (1.89 mg, 0.003 mmol) and 120° 4,4′-[*trans*-Pt(PEt$_3$)$_2$(NO$_3$)$_2$]diphenyl ketone **7** (3.50 mg, 0.003 mmol) were dissolved in 1.0 mL of DMSO-d_6 in a 2 mL dram vial. The reaction mixture was allowed to stir for 8 h at 50 °C. To the resulting homogeneous solution, diethyl ether was added to precipitate the product, which was then isolated and dried under reduced pressure and re-dissolved in DMSO-d_6 for characterization. The ^{1}H NMR spectrum of hexagon **3** is shown in Figure S25. ^{1}H NMR (DMSO-d_6, room temperature, 300 MHz) δ (ppm): 11.40 (s, 3H), 9.55 (s, 3H), 8.85 (d, J = 5.7 Hz, 12H), 7.84 (d, J = 5.4 Hz, 12H), 7.49–7.59 (m, 18H), 7.36–7.48 (m, 18H), 5.70 (s, 3H), 3.97–4.14 (m, 6H), 3.09–3.19 (m, 6H), 1.64–1.81 (m, 6H), 1.39–1.56 (m, 45H), 1.21–1.38 (m, 72H), 0.94–1.13 (m,108H), 0.68–0.83 (m, 18H). The ^{31}P {^{1}H} NMR spectrum of hexagon **3** is shown in Figure S26. ^{31}P {^{1}H} NMR (DMSO-d_6, room temperature, 121.4 MHz) δ (ppm): 10.01 ppm (s, ^{195}Pt satellites, $^1J_{Pt-P}$ = 2638.9 Hz). ESI-MS is shown in Figure S24: m/z 836.85 [M – 6OTf]$^{6+}$, 846.53 [M – 2HNO$_3$ – 4NO$_3$ + Na + K]$^{6+}$, 1004.03 [M – HNO$_3$ – 5NO$_3$]$^{5+}$, 1011.42 [M – 2HNO$_3$ – 4NO$_3$ + K]$^{5+}$, 1016.43 [M – 5NO$_3$]$^{5+}$, 1254.53 [M – 2HNO$_3$ – 4NO$_3$]$^{4+}$, 1263.53 [M – 3HNO$_3$ – 3NO$_3$ + K]$^{4+}$, 1270.54 [M – 4HNO$_3$ – 2NO$_3$ + Na + K]$^{4+}$.

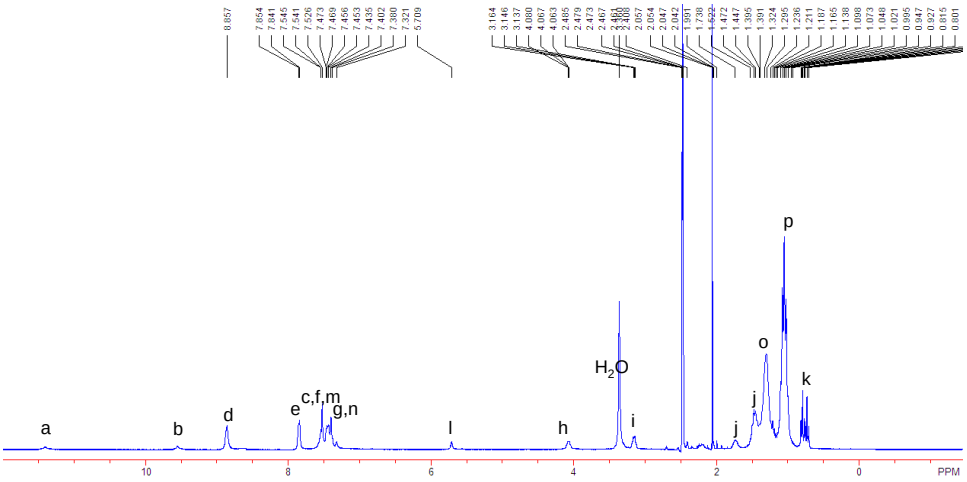

Figure S25. ^{1}H NMR spectrum (DMSO-d_6, room temperature, 300 MHz) of hexagon **3**.

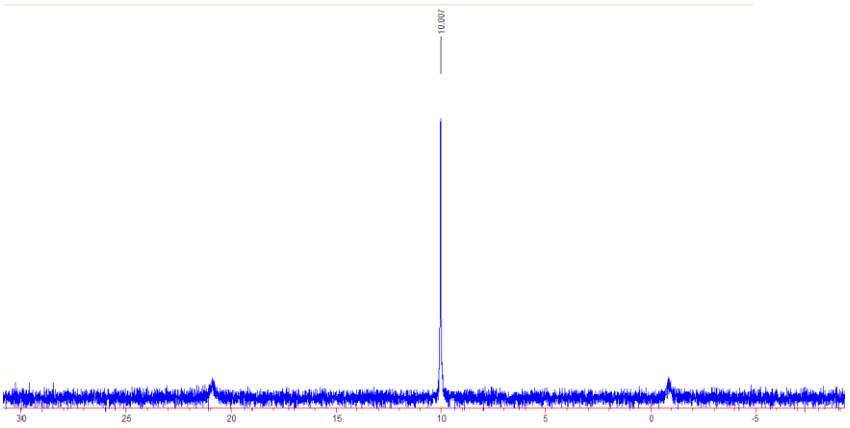

Figure S26. ^{31}P {^{1}H} NMR spectrum (DMSO-d_6, room temperature, 121.4 MHz) of hexagon **3**.

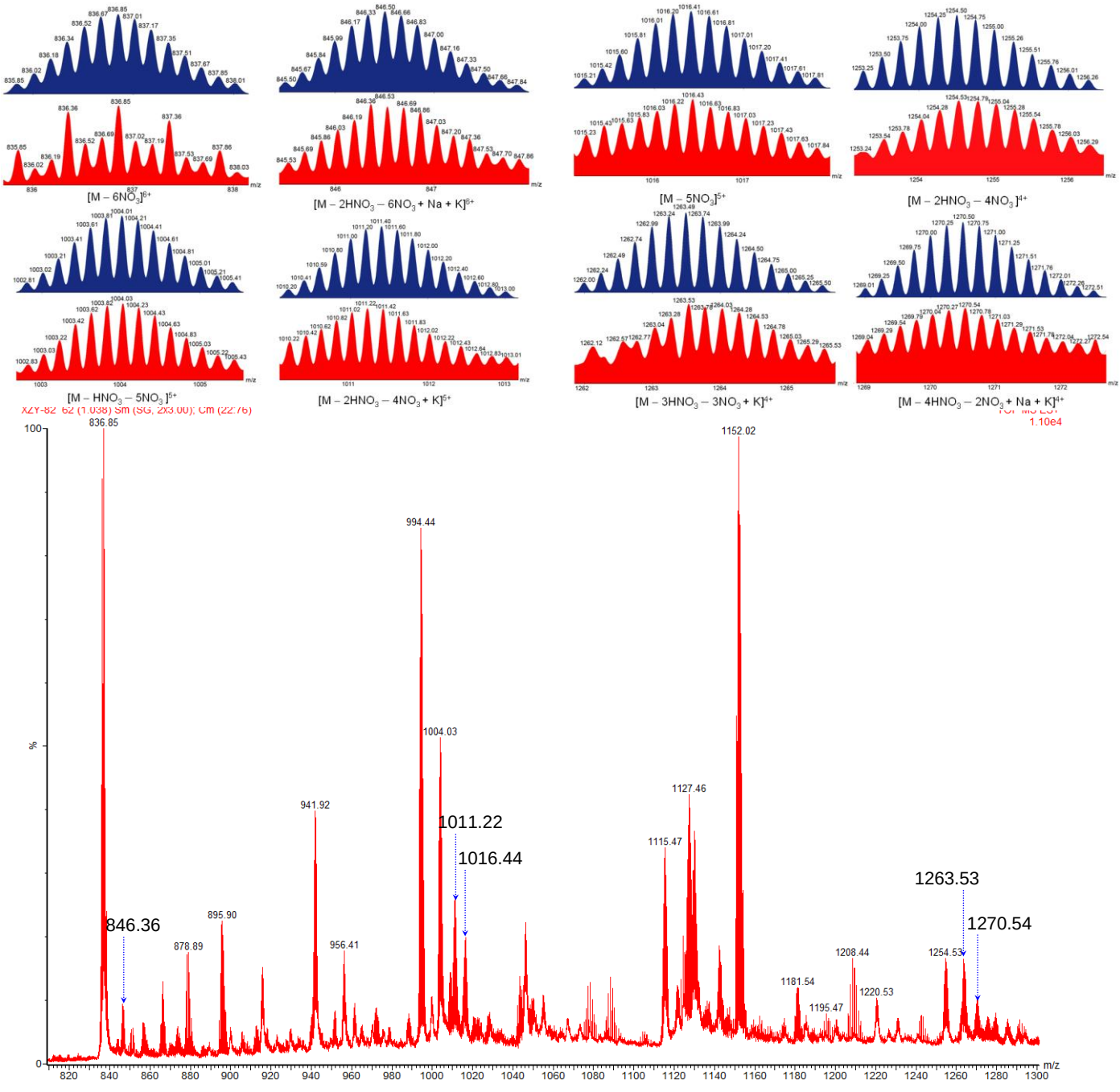

Figure S27. Experimental (red) and calculated (blue) electrospray ionization mass spectrum of hexagon **3**.

Section C. Characterization of Metallosupramolecules

*1. Simulated molecular models of UPy-functionalized rhomboid **1** and hexagons **2** and **3***

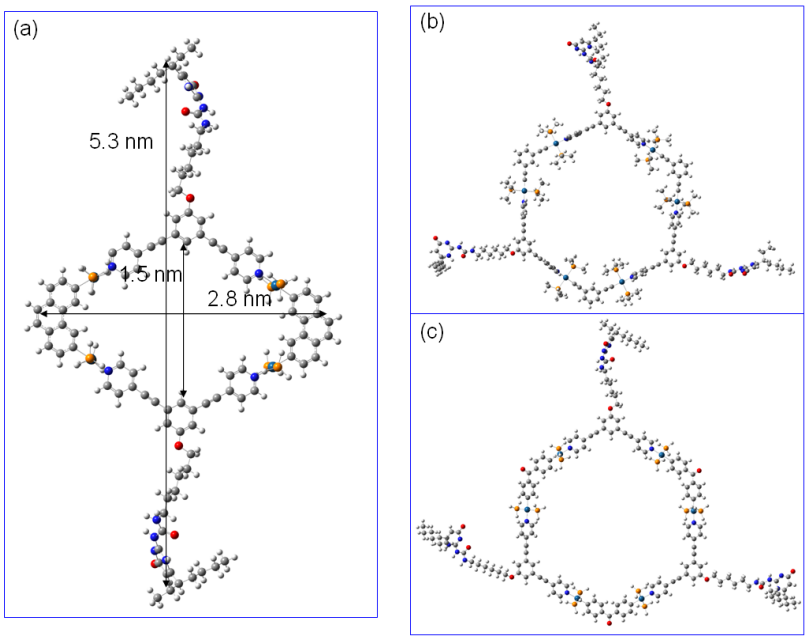

Figure S28. Simulated molecular models of UPy-functionalized rhomboid **1** (a), hexagons **2** (b) and **3** (c) optimized with Molecular Mechanics Universal force field (UFF). Color code: C = gray, H = light gray, O = red, N = blue, P = orange, Pt = green.

Molecular modeling Procedure:

Metallacycles **1**–**3** were constructed and visualized using GaussView 5.0,[S5] and geometry optimizations were performed using Molecular Mechanics Universal force field (UFF)[S6] within the Gaussian 09 package, revision B.01.[S7] A frequency calculation was also performed to determine whether imaginary states exist below the reported minimized energy.[S8] To minimize computational cost, the PEt_3 ligands were modeled as PH_3 for metallacycles **1** and **3**, while $P(CH_3)_3$ was used for metallacycle **2**.

*2. Orthogonal self-assembly of 120° UPy-functionalized dipyridyl ligand **4** and 60° organoplatinum(II) acceptor **5***

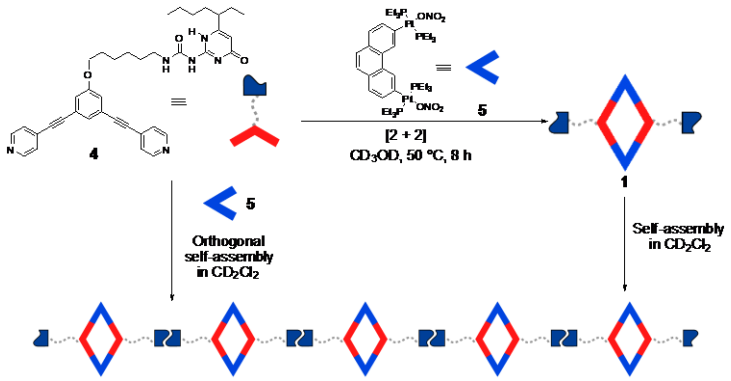

Figure S29. Cartoon representation of two self-assembly routes for the formation of linear supramolecular polyrhombiod.

*3. Concentration-dependent $^{31}P\{^{1}H\}$ NMR spectra of rhomboid **1***

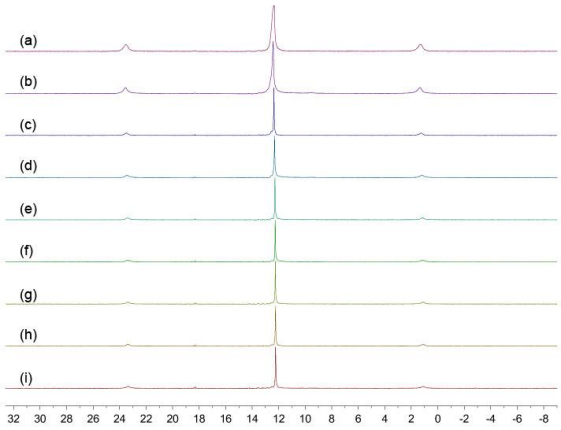

Figure S30. $^{31}P\{^{1}H\}$ NMR spectrum (CD_2Cl_2, room temperature, 121.4 MHz) of rhomboid **1** at different concentrations: (a) 110 mM; (b) 90.0 mM; (c) 78.0 mM; (d) 60.0 mM; (e) 40.0 mM; (f) 34.0 mM; (g) 28.0 mM; (h) 20.0 mM; (i) 15.0 mM.

*4. DOSY NMR experiment of parent rhomboid **15***

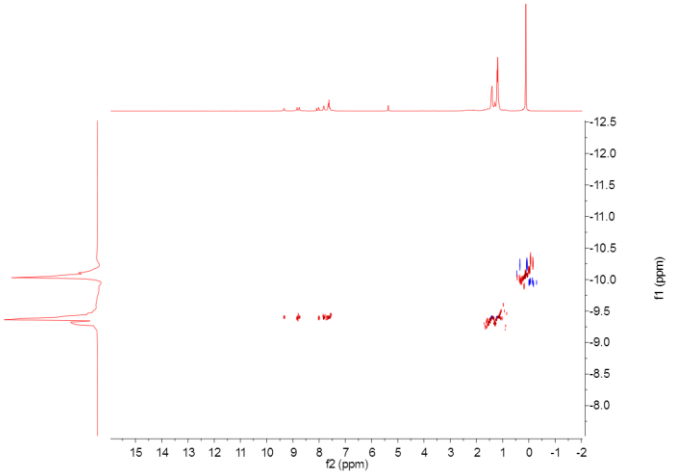

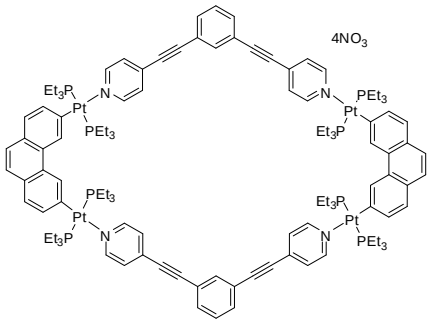

15

Figure S31. DOSY NMR spectrum (CD_2Cl_2, room temperature, 500 MHz) of rhomboid **15** at 20.0 mM.

*5. DOSY NMR experiments of UPy-functionalized rhomboid **1** at different concentrations*

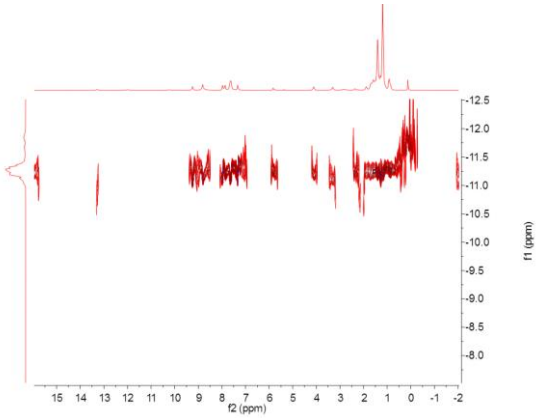

Figure S32. DOSY NMR spectrum (CD_2Cl_2, room temperature, 500 MHz) of UPy-functionalized rhomboid **1** at 90.0 mM.

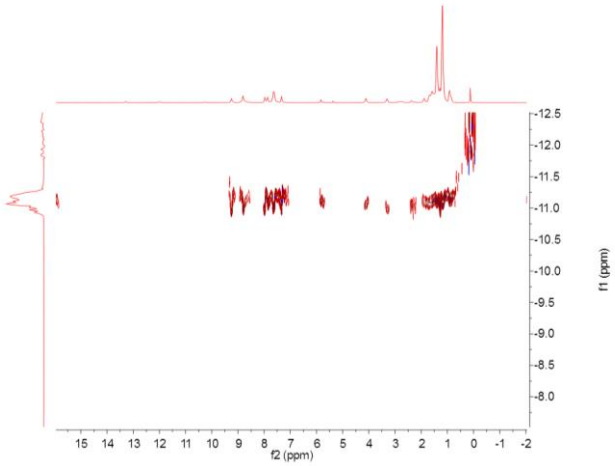

Figure S33. DOSY NMR spectrum (CD_2Cl_2, room temperature, 500 MHz) of UPy-functionalized rhomboid **1** at 75.0 mM.

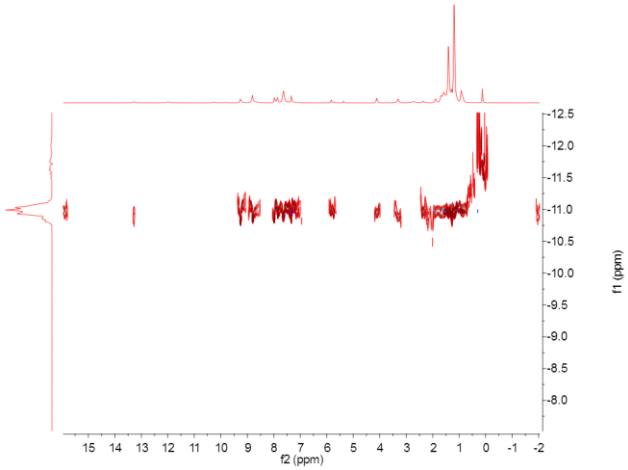

Figure S34. DOSY NMR spectrum (CD_2Cl_2, room temperature, 500 MHz) of UPy-functionalized rhomboid **1** at 65.0 mM.

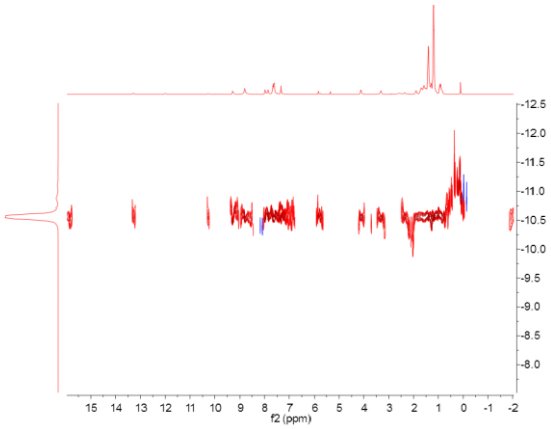

Figure S35. DOSY NMR spectrum (CD_2Cl_2, room temperature, 500 MHz) of UPy-functionalized rhomboid **1** at 40.0 mM.

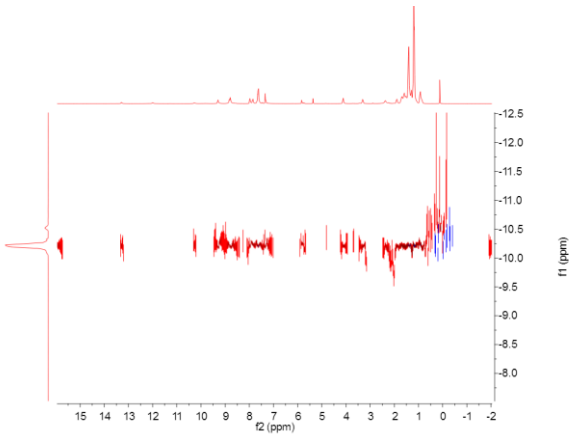

Figure S36. DOSY NMR spectrum (CD_2Cl_2, room temperature, 500 MHz) of UPy-functionalized rhomboid **1** at 20.0 mM.

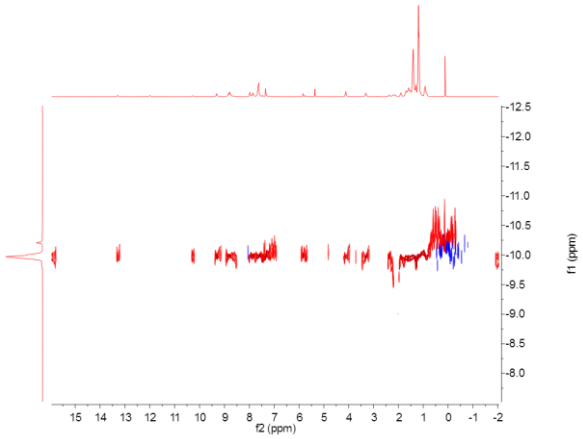

Figure S37. DOSY NMR spectrum (CD_2Cl_2, room temperature, 500 MHz) of UPy-functionalized rhomboid **1** at 10.0 mM.

*6. DLS experiment of parent rhomboid **15***

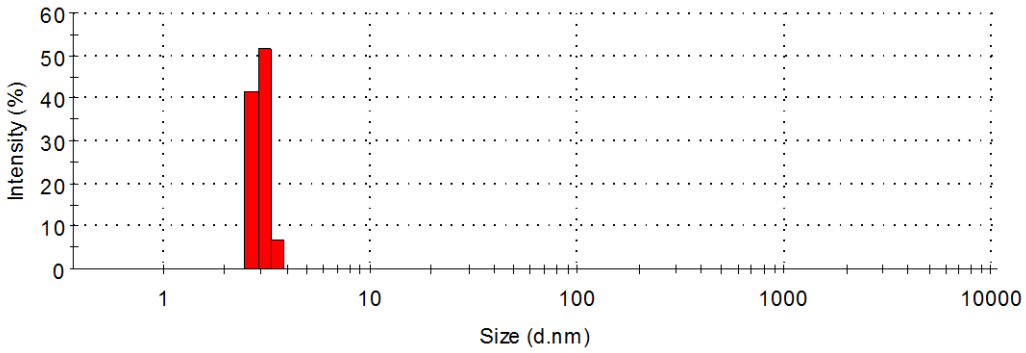

Figure S38. Size distribution of parent rhomboid **15** at 2.00 mM, D_h = 3.14 nm.

*7. FT-IR experiments of 120° UPy-functionalized dipyridyl ligand **4** and hexagons **2** and **3***

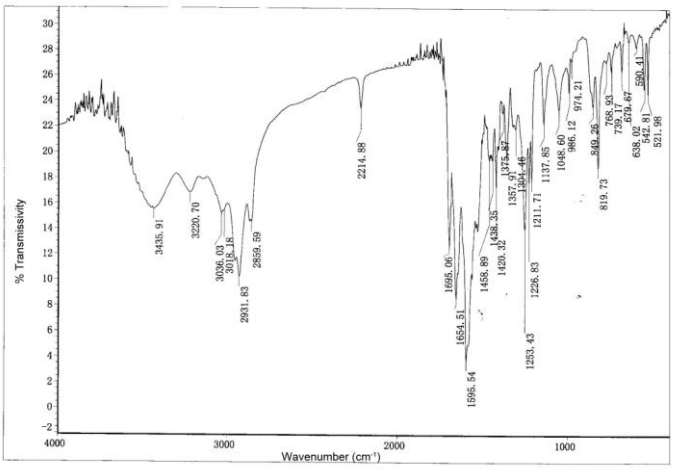

Figure S39. FT-IR (KBr pellets) of UPy-functionalized ligand **4**.

Typical peaks: 3435.91, 1695.06, 1654.51, 1595.54 cm^{-1}, N–H for hydrogen-bonding formation,[S4,9] absence of a 2500 cm^{-1} band for the enol tautomer[S4,9]

2214.88 cm^{-1} for C≡C on the ligand **4**

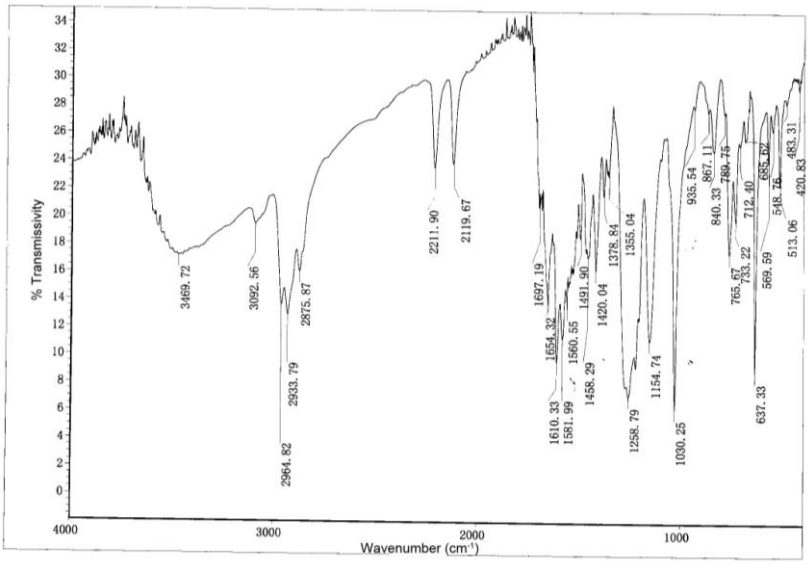

Figure S40. FT-IR (KBr pellets) of hexagon **2**.

Typical peaks: 3469.72, 1697.19, 1654.32, 1581.99 cm^{-1}, N–H for hydrogen-bonding formation,[S4,9] absence of a 2500 cm^{-1} band for the enol tautomer[S4,9]

2211.90 cm^{-1} for C≡C on the ligand

2119.67 cm^{-1} for C≡C on the organoplatinum(II) acceptor

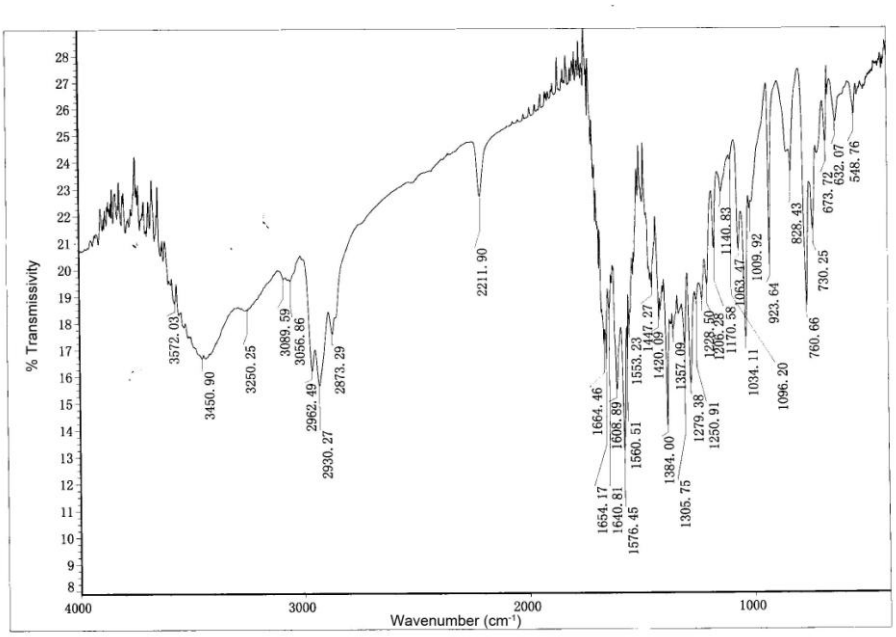

Figure S41. FT-IR (KBr pellets) of hexagon **3**.

Typical peaks: 3450.90, 1664.46, 1654.17, 1576.45 cm^{-1}, N–H for hydrogen-bonding formation,[S4,9] absence of a 2500 cm^{-1} band for the enol tautomer[S4,9]

2211.90 cm^{-1} for C≡C on the ligand

*8. Swelling experiments of hexagons **2** and **3** in dichloromethane*

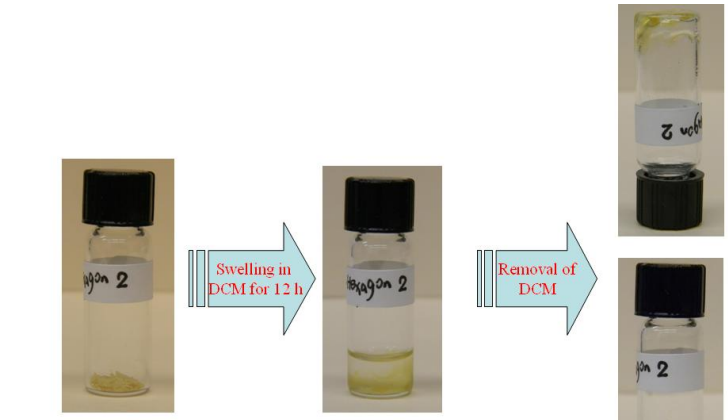

$$Q = \frac{m - m_0}{m_0} = \frac{(95.60 - 14.98)mg}{14.98mg} = 5.38$$

Figure S42. Cartoon representation of the swelling experiment of hexagon **2** in dichloromethane (DCM). Here, Q is the degree of swelling; m is the weight of the swelled sample; m_0 is the weight of the initial sample.

$$Q = \frac{m - m_0}{m_0} = \frac{(143.57 - 15.72)mg}{15.72mg} = 8.13$$

Figure S43. Cartoon representation of the swelling experiment of hexagon **3** in dichloromethane (DCM). Here, Q is the degree of swelling; m is the weight of the swelled sample; m_0 is the weight of the initial sample.

*9. SEM images of rhomboid **1** and hexagons **2** and **3***

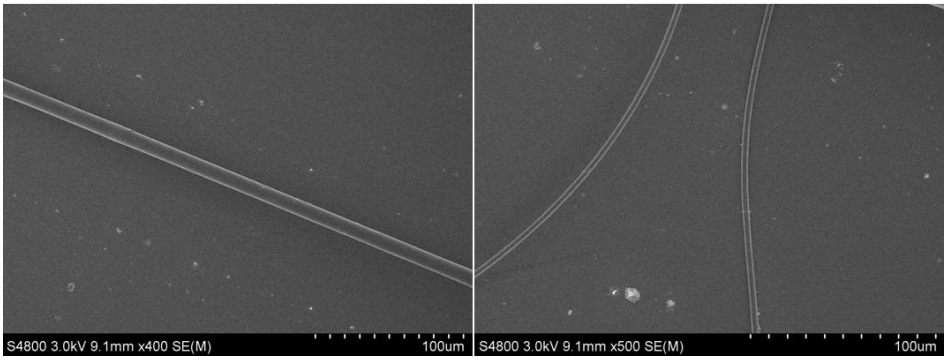

Figure S44. SEM images of rod-like fibers drawn from a high concentrated solution of rhomboid **1** in DCM.

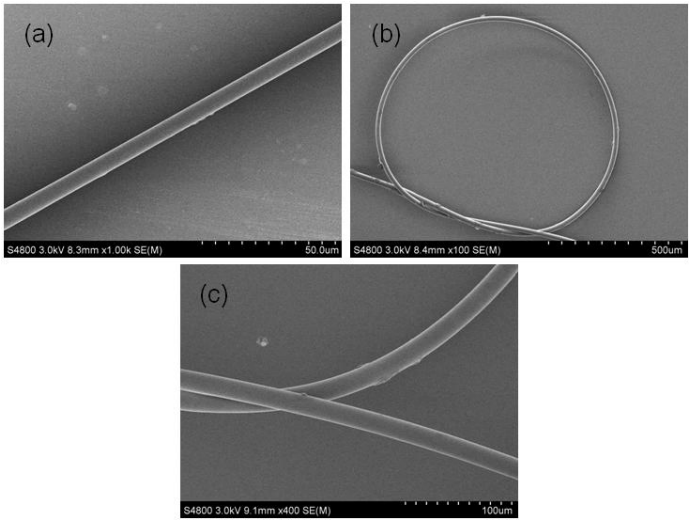

Figure S45. SEM images of (a) a rod-like fiber drawn from the swelled UPy-functionalized hexagon **2**, (b) a knot made from the fiber which was drawn from the swelled UPy-functionalized hexagon **2**, and (c) rod-like fibers drawn from the swelled UPy-functionalized hexagon **3**.

10. Instructions of the attached movie, Video S1

The sample in Video S1 was the swelled hexagon **3**, which was prepared by swelling in dichloromethane overnight. The solvent in the vial was dichloromethane. In the movie, 0–18 s showed the process of drawing fiber from the swelled hexagon **3** and 19 s–1 min 03 s showed the stretchability and flexibility of the resultant fiber. As shown in the movie, the fiber was too thin to see (so you need to focus) and can flutter driving by breeze like long hair. According to our observation, the fiber can keep its flexibility even overnight.

Section D. References

S1. Yang HB, Ghosh K, Arif AM, Stang PJ (2006) The synthesis of new 60° organometallic subunits and self-assembly of three-dimensional M_3L_2 trigonal-bipyramidal cages. *J Org Chem* 71: 9464–7469.

S2. Yang HB, et al. (2007) A highly efficient approach to the self-assembly of hexagonal cavity-cored tris[2]pseudorotaxanes from several components via multiple noncovalent interactions. *J Am Chem Soc* 129: 14187–14189.

S3. Li SL, Xiao T, Wu Y, Jiang J, Wang L (2011) New linear supramolecular polymers that are driven by the combination of quadruple hydrogen bonding and crown ether–paraquat recognition. *Chem Commun* 47: 6903–6905.

S4. Beijer FH, Sijbesma RP, Kooijman H, Spek AL, Meijer EW (1998) Strong dimerization of ureidopyrimidones via quadruple hydrogen bonding. *J Am Chem Soc* 120: 6761–6769.

S5. http://www.gaussian.com/g_tech/gv5ref/gv5citation.htm

S6. Rappe AK, Casewit CJ, Colwell KS, Goddard III WA, Skiff WM (1992) UFF, a full periodic table force field for molecular mechanics and molecular dynamic simulations. *J Am Chem Soc* 114: 10024–10035.

S7. Frisch MJ, et al. (2010) *Gaussian* (Gaussian, Inc.: Wallingford, CT).

S8. Pollock JB, Cook TR, Stang PJ (2012) Photophysical and computational investigations of bis(phosphine) organoplatinum(II) metallacycles. *J Am Chem Soc* 134: 10607–10620.

S9. Li SL, et al. (2011) New light on the ring-chain equilibrium of a hydrogen-bonded supramolecular polymer based on a photochromic dithienylethene unit and its energy-transfer properties as a storage material. *Chem Eur J* 17: 10716–10723.